A pilot plant investigation on real seawater brine valorisation via electrodialysis with bipolar membranes

Giovanni Virruso[†], *Calogero Cassaro*[†], *Fabrizio Vassallo, Antonia Filingeri, Alessandra Pellegrino, Alessandro Tamburini*[*], *Andrea Cipollina, Giorgio Micale*

Dipartimento di Ingegneria, Università degli studi di Palermo, Viale delle Scienze Ed.6, Palermo, 90128, Italia

[†] These authors equally contributed to the work.

*Corresponding author. Tel: +39-3920592179. E-mail: alessandro.tamburini@unipa.it (Alessandro Tamburini)

Keywords: Brine mining, BMED, ion-exchange membrane, water-splitting electrodialysis, scale-up.

Abstract

Environmental concerns related to industrial wastewater streams can be minimized employing zero/minimum liquid discharge strategies, recovering high-value materials to make them economically competitive. However, suitable reactants, such as acid and alkaline solutions, are necessary. To this aim, Electrodialysis with Bipolar Membranes (EDBM) can be employed to *in-situ* produce chemicals. This work studies a semi-industrial scale EDBM unit, fed by either a real seawater brine or a synthetic NaCl solution. Risk mitigation approaches adopted to guarantee continuous operation are described. EDBM performance, as operating conditions vary, is evaluated under two control strategies (i.e., flowrate and pressure control). The pressure control strategy guarantees higher performance, minimizing undesired convective fluxes. Values of current efficiency and specific energy consumption of 68% and 2.4 kWh kg^{-1}, respectively, were obtained for the alkaline product

at 1.1 mol L^{-1} concentration. Multi-ion transport within membranes is evaluated under pressure control strategy. The analysis highlights a dominant passage of Cl^{-1} and Na^{+} in the acid and alkaline stream, respectively, resulting in products containing > 90% of Cl^{-1} (acid stream) and > 98% of Na^{+} (alkaline stream). These results proved the attractiveness of EDBM process in treating real brine to produce acid and base solutions.

1 Introduction

Increasing resources demand along with more strictly water policies are promoting the transition towards circular production systems [1,2]. Sustainable water management approaches are required by industries (i) to minimize wastewater volumes and their associated environmental impact [3], and (ii) to reduce water consumption [4]. To this end, minimal liquid discharge (MLD) [5] and zero liquid discharge (ZLD) [6] strategies have been proposed. These strategies aim to valorise wastewater, recovering useful materials and freshwater (up to 90–95%), instead of being disposed of [7]. Two different treatment approaches are usually adopted in MLD and ZLD strategies for the concentration of salt solutions: MLD mainly integrates membrane-based processes, while ZLD employs both membrane-based and thermal-based technologies [5]. In general, thermal–based processes are more expensive compared to membrane-based ones, due to the high capital investment and to the elevated energy consumption [8], but they can reach saturation in the outlet brine. On the contrary, several pretreatment steps are required prior to a membrane process to reduce fouling phenomena that severely affect their performance [9], while lower recovery is obtained.

A primary important aspect to widespread MLD and ZLD treatment chains is to make them economically competitive, beside to the environmental benefits. This can be achieved by recovering valuable resources (i.e., salts, minerals, chemicals, etc) that can be sold or reused *in-situ*.

Thermal crystallizers are often employed to recovery high purity salts, such as sodium chloride, sodium sulphate [10] and calcium sulphate [11], or a mixture of salts [12] that can be used in agriculture.

To recover high-value materials, such as magnesium, lithium, boron and chromium, reactive precipitation or selective absorption/adsorption is needed [13–16], thus requiring the use of chemical reagents. Among them, acid and base streams such as sodium hydroxide and hydrochloric acid, represent the mostly used. As an example, sodium hydroxide is employed in the field of brine valorisation to produce $Mg(OH)_2$ and $Ca(OH)_2$ from waste salt solutions using innovative crystallizers [13]. Lithium and boron can be simultaneously recovered from brines thanks to the

collaborative absorption in Lithium-Ion sieves and Boron chelating resins [15]. The regeneration of sieves and resins is accomplished using 0.3 mol L^{-1} HCl. Another example regards the recovery of chromium (in the form of Cr^{6+}) from electroplating wastewaters by ion exchange resins (silica-supported pyridine resin) [16], which requires, as resins' eluent solutions, 1 mol L^{-1} NaOH or 1 mol L^{-1} HCl, while for the regeneration of the resins 0.1 mol L^{-1} HCl is employed.

Thus, generating *in-situ* acid and alkaline solutions from waste brine is essential to guarantee the economic and environmental sustainability of ZLD and MLD strategies. ElectroDialysis with Bipolar Membranes (EDBM) can be interestingly used to produce chemicals solutions from waste saline streams [17]. In this way, industrial processes can benefit from both economic and environmental improvements.

EDBM is an electro-membrane process enabling the simultaneous production of acid and alkaline streams, desalting a salt solution [18]. The process utilises ion-exchange membranes (anionic (AEM) and cationic (CEM) exchange membrane), as well as bipolar (BM) membranes. The latter component makes the chemicals production possible. BM consists of the overlapping a cationic and an anionic layer [19]. Catalysts such as metal hydroxides or tertiary amine groups [20,21] are employed to promote water dissociation reaction inside the bipolar membrane interlayer. The repetitive unit of an EDBM stack, named triplet, is composed of the three different membranes and of three spacer-filled channels (i.e., acid, base and salt channels) [22]. For industrial units, up to 200 triplets can be installed in single stack [23]. Typically, the salty solution is sent to the salt channel, while water is used as input for the acid and base compartments. The cells pack is placed between a couple of electrodes and an electrical potential difference is established, generating an electric field. This promotes the water-dissociation reaction inside the BM and the migration of ions toward the opposite charged electrode [24]. Cations easily permeate through CEMs, while they are retained by AEMs thanks to Donnan exclusion effect. Similarly, anions pass through AEMs and are blocked by CEMs. The basic concept of an EDBM unit is represented in the supplementary information (Figure S1).

According to the scientific literature, the EDBM process has been applied in a variety of fields, such as in the production of organic [25] and inorganic acids and bases [26], in the capture of CO_2 [27] and in brines valorisation [28], even on a semi-industrial scale [29].

Concerning the valorisation of different waste saline solutions, Adiba et al. in 2023 [30] proposed a multi-stage membrane integrated system for the treatment of high-salinity NaCl and Na_2SO_4, emulating a coal mining wastewater from Bulianta (China). In this study, the authors investigated two different combinations for an integrated chain combining Reverse Osmosis (RO), Nano Filtration (NF), Electrodialysis (ED) and EDBM. Regarding EDBM, a laboratory unit, with membranes supplied by Hangzhou Lanran Technology Co. Ltd (China), was used employing artificial Na_2SO_4 and NaCl/Na_2SO_4 mixed solutions and a current density up to 300 A m^{-2}. The results showed a minimum Specific Energy Consumption (SEC) of 65 Wh $mol_{OH^-}^{-1}$ (~1.6 kWh kg_{NaOH}^{-1}), obtained with 1.4 mol L^{-1} NaCl concentration and a 1:20 mole ratio with Na_2SO_4. The highest concentration of acid and base produced were 0.95 mol L^{-1} and 1.5 mol L^{-1}, respectively.

In the work of Peng et al., 2023, [31], the authors adopted the EDBM process for the valorisation of carbocysteine (H2ccys) wastewater, which contains H2ccys, chloroacetic acid, and ammonium chloride, which could represent significant risks to the environment. Specifically, the study used EDBM stacks, from laboratory to pilot scale, supplied from FuMA-Tech GmbH (Germany), for the purification and production of 1.33–1.63 mol L^{-1} HCl and 2.62–2.88 mol L^{-1} $NH_3 \cdot H_2O$. Almost all the H2ccys molecules were retained in the salt solution and about 80% of them were recovered. The authors investigated a two-stage EDBM pilot plant optimised to minimise the thermal effect on the stack external circuit. The results revealed, with a current density of 500 A m^{-2}, a Current Efficiency (CE) of about 50% and a SEC in the range of 3.60–4.09 kWh kg_{NaOH}^{-1}, obtained during nine days of testing. In the work of Jiang et al. in 2021 [32], the possibility of combining RO, ED and EDBM was proposed for salt concentration as well as acid and base production from cold-rolling wastewater. The feed stream to EDBM was previously concentrated by a RO unit and a double stage ED process. The concentrated salty solution, containing mainly Na_2SO_4, is then used to produce sodium hydroxide and

sulfuric acid via EDBM. A laboratory scale stack with 5 triplets and an active membrane area of 189 cm^2, supplied by ASTOM Co. (Japan), was used in closed-loop. Maximum acid and base concentrations of 2.35 mol L^{-1} and 2.03 mol L^{-1}, respectively, were registered for a volume ratio of salt:acid:base equal to 5:3:3. In 2023, Zhao et al. [33] aimed at the valorisation of mine water generated during coal extraction. In detail, the work proposed an integrated process of: (i) Ultra Filtration (UF) and RO, to filter and concentrate the wastewater, (ii) Selectrodialysis (SED), for multivalent ion separation in the concentrated wastewater, and (iii) EDBM to convert the purified brine, containing Na_2SO_4 and NaCl, into acids and bases, with the goal of achieving ZLD and resourceful treatment. The EDBM utilized monopolar membranes (i.e., CEM and AEM) supplied from Hangzhou Lanran Technology Co. Ltd and BP provided by ASTOM Co. (Japan). The stack was operated with a current density of 200 A m^{-2}, achieving a 67 % CE and about 3.1 kWh kg_{NaOH}^{-1} SEC at alkaline concentration of 0.77 mol L^{-1}.

Regarding specific EDBM applications to seawater brine valorisation, several works are available. Reig et al in 2016 a [26] combined NF and EDBM to concentrate Mg^{2+} and Ca^{2+} as well as to produce acid and alkaline streams from a seawater RO brine. The EDBM unit, which employed PCCell GmbH (Germany) membranes, was fed with artificial NaCl (representing the permeate NF after a precipitation step to further remove bivalent ions). A closed-loop configuration was adopted, reaching NaOH and HCl concentration of about 1 mol L^{-1} at constant voltage (9V). A SEC of 2.6 kWh kg^{-1} and CE of 77% were registered for NaOH. In another work, Reig et al. in 2016 b [34], integrated ED and EDBM to valorise seawater RO desalination brine into chemicals. The same EDBM stack was fed with synthetic sodium chloride solutions and operated in closed loop with current densities of 300–400 A m^{-2}. Acid and base concentrations of 0.66–2.2 mol L^{-1} were achieved, with SEC ranging from 1.7 to 3.8 kWh kg_{NaOH}^{-1} and 80 % maximum CE. In 2023, Filingeri et al. [35] tested a lab-scale EDBM stack, with membranes supplied by SUEZ (France), for the valorisation of an artificial multi-ionic solutions, mimicking solar saltworks bitterns from Trapani (Italy). Tests were carried out at 300 A m^{-2}, and a NaOH solution with a concentration in the range of 1.15–1.44 mol L^{-1} was produced.

Improvements in EDBM performance indicators were observed when multi-ion solutions were fed to the salt compartment, resulting in CE of 70–80 %, and SEC in the range 1.42–1.75 kWh kg_{NaOH}^{-1} with 0.5 mol L^{-1} NaOH target production, while in the range 1.60–1.94 kWh kg_{NaOH}^{-1} with 1 mol L^{-1} NaOH target.

Although the EDBM process has been extensively tested on lab scale with synthetic solutions, only a few works employed real solutions [26,31–33,36], for which several pretreatments are needed. In addition, the adopted stacks present a small total membrane area and a low number of triplets, which has a beneficial effect on the performance (e. g., parasitic currents can be neglected). In all the previous works, batch configuration (closed-loop) are employed and no information can be found about the continuous operation of EDBM systems for several hours, especially with real solutions. Table S1 summarises the key information and compare previous work with the present work. Based on the above considerations the aim of this work has been to assess and present, for the first time in the open literature, the performance of a large scale EDBM pilot plant (19.2 m^2 of total membrane area) operated in continuous mode (feed and bleed process configuration) and fed by a real saline solution (seawater brine). Pretreatment steps required and precautions taken to safely operate the system are described in detail. A long run test of 59 h of continuous operation was conducted switching from artificial to real solutions. The differences between the two solutions were evaluated adopting the main key performance indicators (KPIs) of the EDBM process. Moreover, two different control strategies were employed during the test (flowrate control and differential pressure control) and several steady-state conditions were evaluated for each strategy. Finally, the pressure control strategy, which guarantees the best performance, was further investigated to assess the behaviour of different ions in terms of their apparent transport number and selectivity of the membranes.

2 Materials and methods

2.1 Brine treatment chain and EDBM feed characterization

The EDBM pilot plant is part of an integrated treatment chain realized in the framework of the European Horizon 2020 Water-Ming project [37] and installed in the island of Lampedusa (Italy). The aim of the project is to valorise saline streams (seawater or desalination brine) recovering fresh water, chemicals (i.e., acid and base streams), salt (i.e., sodium chloride and mixed salts) and minerals (i.e., $Mg(OH)_2$, $Ca(OH)_2$), adopting technologies at high technology readiness level (TRL, in the range 5-7). This treatment chain applies a ZLD strategy employing six different technologies: (i) Nano Filtration (NF), (ii) Multiple Feed Plug Flow Reactor (MF-PFR), (iii) Multiple Effect Distillation (MED), (iv) ElectroDialysis with Bipolar Membrane (EDBM), and (v) Evaporative Ponds (EPs). A representation of the whole treatment chain is illustrated in Figure 1.

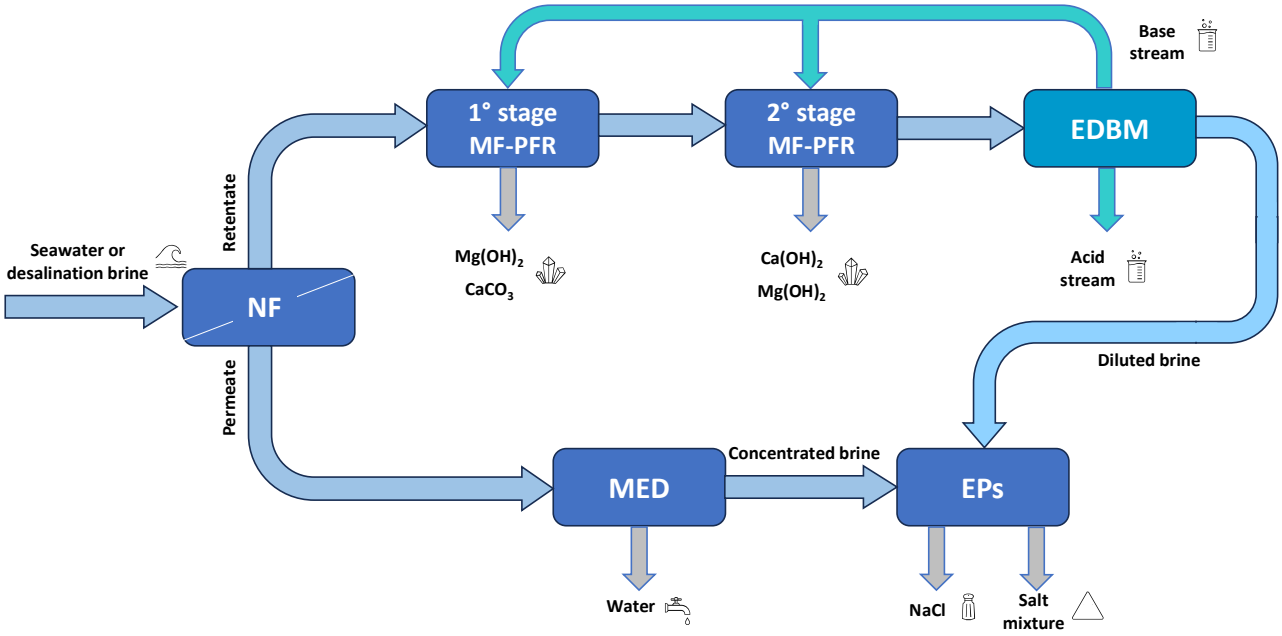

Figure 1. Schematic representation of the European Horizon 2020 Water-Mining project treatment chain for the valorisation of seawater brines.

The inlet saline feed is firstly treated in a NF unit, a membrane process which produces: i) a permeate, containing mainly monovalent ions (such as, sodium, potassium and chloride) and ii) a retentate,

enriched in bivalent ions (such as, magnesium, calcium and sulphates). The NF retentate is sent to an innovative reactive crystallizer, known as MF-PFR, employed in two different stages. The first stage recovers a mixture of magnesium hydroxide and calcium carbonate (in small quantity), utilising sodium hydroxide as chemical reagent. The second stage operates at a higher pH to precipitate a mixture of calcium/magnesium hydroxide. After solid separation the resulted clarified solution underwent a polishing step with ion exchange resins (IX), further details are provided in section 2.3. The obtained solution is sent to the downstream EDBM unit to produce two chemical streams: (i) an alkaline solution, mainly containing sodium hydroxide, which is recirculated inside the chain for the precipitation steps, and (ii) an acid solution, mainly containing hydrochloric acid, which is partially used for cleaning procedures or as by-product.

The NF permeate is fed to a Multi Effect Distillation (MED) unit to further concentrate the salty stream and to produce demineralized water. The MED unit employs low grade heat (~80°C) supplied by the local power station, achieving a concentration factor as high as 8. The highly concentrated salty solution, produced by the MED unit, along with the diluted brine from the EDBM are directed to the Evaporative Ponds where natural evaporation is employed to crystalise sodium chloride (food grade purity) and a final mixture of other salts (mainly KCl, NaCl and Na_2SO_4).

In this work, seawater was used as feed for the chain and the resulting composition of the salt solution fed to the EDBM unit is reported in Table 1.

Table 1. Composition of the real brine fed to the EDBM unit.

Brine	**Average Salt concentration (mol L^{-1})**					**Conductivity (mS cm^{-1})**
	Na^+	**K^+**	**Cl^-**	**SO_4^{2-}**	**OH^-**	
Real	0.72 ± 0.03	0.01 ± 0.001	0.52 ± 0.02	0.055 ± 0.004	0.100 ± 0.02*	67±2**
Synthetic	0.75± 0.03		0.75± 0.03			67±2**

*Corresponding to a pH in the range 12.9–13.1.
**Conductivity measured at 20°C

2.2 EDBM unit description

The EDBM stack employed in this work is an FT-ED 1600-3-40-2 unit purchased from FuMA-Tech GmbH (Germany). The unit has an internal staging configuration with two cell packs (20 triplet each), with a total membrane area of 19.2 m^2. The membranes installed in the EDBM stack are FUMASEP® FAB-PK as anion-exchange membrane, FUMASEP® FKB-PK as cation-exchange membrane, FUMASEP® FBM-PK as bipolar membranes and FUMASEP® F-10150-PTFE as end-membrane. The active membrane area is 0.16 m^2 (0.345 m long and 0.454 m wide). Additional information about the properties of the ion-exchange membranes adopted is reported in the supplementary material (Table S2). A dimensionally stable anode (DSA®) and stainless steel cathode (AISI 304) were used in the EDBM unit. Polypropylene spacers with a thickness of 350 μm are utilized in the stack. Both cell packs are subjected to the same electric potential difference, utilizing a shared anode (i.e., the positive electrode) and two distinct cathodes (i.e., the negative electrodes). Additional information about the stack features can be found in our previous article [38].

2.3 Process configuration and risk mitigation strategies

Aiming to evaluate the feasibility of employing the EDBM pilot plant in the treatment chain presented in Figure 1 and to study his behaviour as the operative conditions vary, the unit was tested in a long-run experience of 59 h. The EDBM pilot was operated in feed and bleed configuration (continuous operating mode) for acid, alkaline and saline streams, while the Electrode Rinse Solution (ERS) was operated in a closed-loop fashion. Figure 2 shows the Process Flow Diagram (PFD) of the EDBM plant. The feed and bleed configuration enables to operate the EDBM in a continuous mode, through the recirculation of a part of the outlet streams to the inlet, using electrically actuated valves (VKDIV/CE DN15, made in PP, FIP® Formatura Iniezione Polimeri S.p.A.). In this way, the residence time of solutions inside the stack is increased and high concentrated chemicals can be produced, keeping a good flow regime inside the channels. Total flowrates entering the stack were controlled

by magnetically-driven centrifugal regenerative turbine pumps (PTM 2.5x6, Teorema S.r.l.), while the outlet flowrates from the system were controlled by gear pumps (FG200-300, Teorema S.r.l.) or electrically driven valves (VKDIV/CE DN15, made in PP, FIP® Formatura Iniezione Polimeri S.p.A.) depending on the outlet flowrate value (1.2 L min^{-1} is split-range value). For flowrate values lower than then 1.2 the gear pump was utilised, whilst for higher values both final control elements were used [39]. Throughout the test, the acid and base compartments were fed with reverse osmosis permeate (~350 μS cm^{-1}). In the ERS compartments, a synthetic solution of sodium sulphate (technical grade, CR GRUPO CRIMIDESA) with a concentration of 0.25 mol L^{-1} was adopted. This solution was pumped through the stack with a constant flowrate of 20 L min^{-1} during the whole test. It is worthy of note how the knowledge gained from previous experimental campaigns, conducted with artificial solution, were utilized to implement safety strategies for risk prevention that could occur during long-run operation, especially with real solutions. Indeed, risk mitigation in an EDBM pilot plant is a critical aspect to ensure the successful and safe operations. The strategy regarded the identification of potential hazards such as membrane fouling, voltage fluctuations, and material degradation.

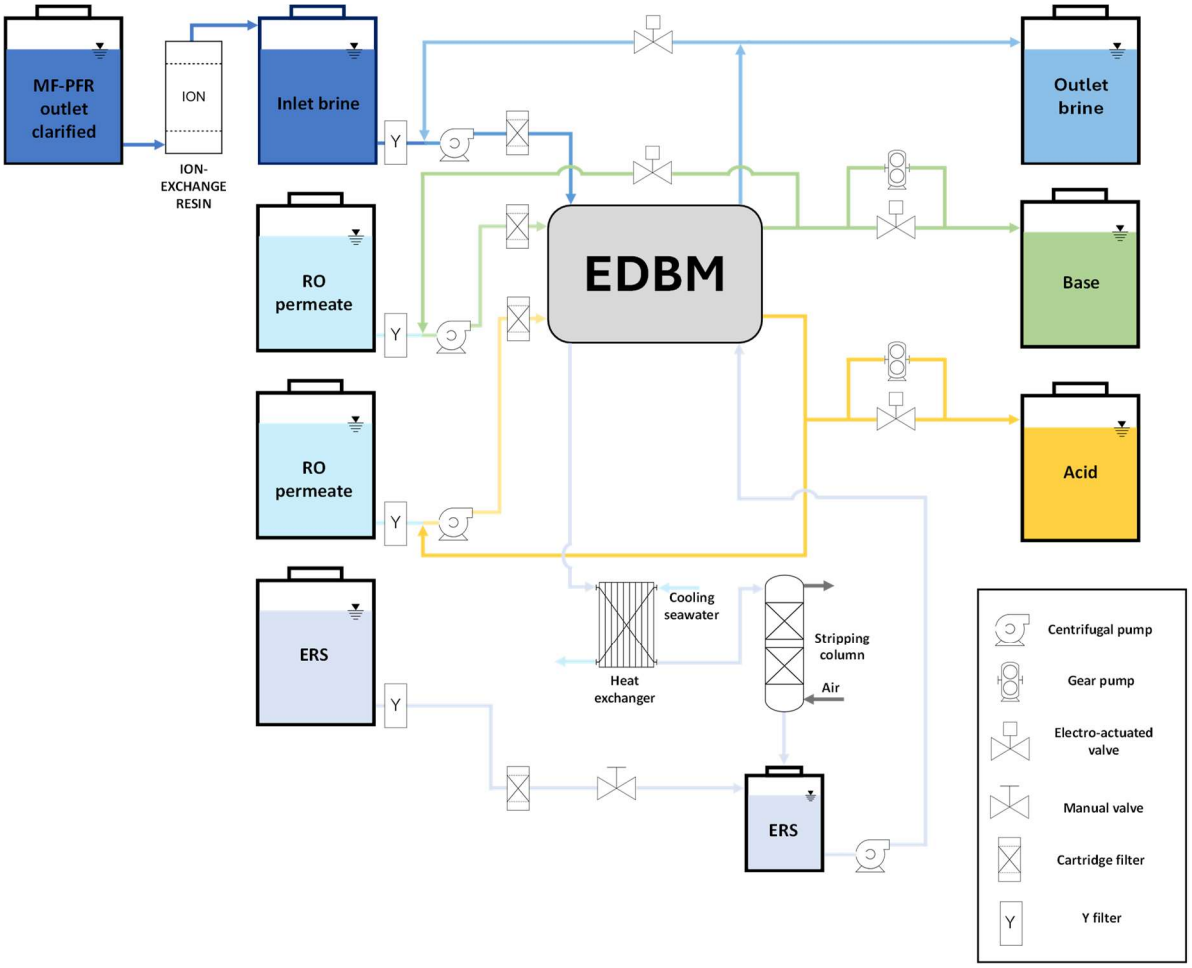

Figure 2. Process Flow Diagram (PFD) of the EDBM pilot plant.

Firstly, ion-exchange resins (IEX), Purolite® C104 Plus, were employed as pretreatment step to ensure that the content of calcium and magnesium ions was always lower than 10 ppm ($CaCO_3$ equivalent), as suggested by the EDBM stack supplier. In fact, a higher concentration of these species could lead to scaling phenomena via precipitation of magnesium and calcium hydroxide in the alkaline compartment causing the clogging of the channels and damaging of membranes. Subsequently, to prevent the voltage from reaching high values during transitory phases, a safety switch-off of the plant was introduced in the programmable logic controller (PLC) avoiding the voltage to exceed 80 V, considered as a safety limit. Moreover, the DC drive implements an additional safety measure to improve the electrical safety of the system. Specifically, the applied potential difference is placed between the ground potential (i.e., a voltage difference of 50 V is obtained, utilizing the anode and

cathode at values of 25 V and -25V, respectively, respect to the ground potential), to reduce the maximum absolute operating voltage of the electrodes compared to the ground potential.

To ensure the stability and the optimal performance of the pilot system, a distinctive strategy was devised for the electrode rinse compartment. Indeed, a titanium plate heat exchanger, cooled by seawater, was introduced to keep the temperature in the electrochemical compartment lower than 40 °C. This was of primary importance as the temperature of the ERS tends to naturally rise, due to Joule effect dissipations, especially when the unit is operated in closed-loop mode. Uncontrolled temperature can lead to thermal degradation of membranes and spacers.

Furthermore, the accumulation of small quantities of chloride ion within the ERS could generate chlorine compounds via competitive reactions at the anode surface, which may provoke long-term chemical damaging of the stack components. To overcome this problem, a stripping column for the degassing of gaseous compounds, such as hydrogen, oxygen and chlorine, from the ERS was installed (Figure 2). Free chlorine content in the ERS was monitored every 2 h and the solution was replaced either when the concentration of free chlorine reached a value greater than 10 ppm or at least every 6 h. Finally, a 3/4 inch polypropylene y-strainer filter (FIP® Formatura Iniezione Polimeri S.p.A.) and a cartridge filter with a 1 μm mesh (Atlas Filtri S.r.l.) were installed to retain coarse particles in the pilot circuit.

These integrated measures ensured the longevity and guarantee high performance of the EDBM process.

2.4 Implemented Control strategies

This section describes the two distinct control strategies adopted during the test.

The flowrate control strategy is implemented to maintain equal velocities in the channels and is widely adopted in lab scale applications [35,40] due to its simplicity of implementation. In this case, a fixed flowrate of 5 L min^{-1} (corresponding to a channel velocity of 2.7 cm s^{-1}) is used for acid, base and salt stream under flowrate control strategy. However, due to inherent differences in pressure

losses within the compartments, this results in unequal pressure distribution among the channels. This pressure difference generates convective flows between the compartments [23], that can lead to neutralization of the produced chemicals, thus reducing the performance of the system.

The pressure control strategy allows to minimise this effect, since equal inlet pressures are imposed in the acid, base, saline and ERS compartments (all the outlet pressures are atmospheric). This approach requires to different recirculation flowrates for acid, base and salt solutions (operated in feed and bleed mode) and, consequently, different velocities within the channels to maintain the same inlet pressure. These two different control strategies were investigated and compared by analysing the system performance under various operating constraints.

2.5 Test description

During the long-run test, the EDBM pilot plant performance was evaluated under different operating conditions and control strategies, employing both an artificial and a real brine. The operating conditions were varied by either acting on the current density supplied to the stack or changing the outlet flowrate of the acid, base and salt stream.

The test lasted 59 h, processing approximately 6 m^3 of real brine and 500 L of synthetic solution. Three step variations in the unit operation were investigated during the test: i) from artificial to real brine, ii) from flowrate control to pressure control strategy and iii) from real to artificial brine. Table 2 summarizes the different phases of the test carried out.

Table 2. Overview of the long-run test conducted with the EDBM pilot plant.

Test phase	Solution	Duration (h)	Collected samples	Control strategy
1	A	3.0	5	F
2	R	29.0	23	F
3	R	24.3	17	P
4	A	2.7	3	P
Total		59.0	48	

A = artificial brine, R = real brine, F = flowrate control mode, P = pressure control mode

Most of the test was conducted employing the real brine in order to demonstrate the stability of the system in a real operational environment. The different operating conditions are codified and summarized in Table 3. The code comes from the acid, base and salt outlet flowrates as well as the current density adopted.

Table 3. Different sets of operating conditions tested with the EDBM pilot plant.

Operating condition code	Solution	Outlet flowrate (L min^{-1})			Current density (A m^{-2})	Control strategy
		Acid	Base	Salt		
1–0.7–1.8–400*	A	1	0.7	1.8	400	F/P
1–0.7–1.8–400	R	1	0.7	1.8	400	F
1–0.8–1.8–400*	R	1	0.8	1.8	400	F/P
1–0.8–2.3–400	R	1	0.8	2.3	400	F
1–0.8–1.8–200	R	1	0.8	1.8	200	F
1–0.8–0.9–200	R	1	0.8	0.9	200	F
2–1.6–1.8–400	R	2	1.6	1.8	400	F
2–1.6–2.3–400	R	2	1.6	2.3	400	F
1.4–1.1–1.8–400	R	1.4	1.1	1.8	400	P
1.4–1.1–2.3–400	R	1.4	1.1	2.3	400	P
1.4–1.1–1.8–200	R	1.4	1.1	1.8	200	P
1.2–1–1.8–400	R	1.2	1	1.8	400	P
1.5–1.1–1.8–400	R	1.5	1.1	1.8	400	P
1.5–1.1–2.3–400	R	1.5	1.1	2.3	400	P

A = artificial brine, R = real brine, F = flowrate control mode, P = pressure control mode.
*both flowrate and l pressure control strategies were investigated.

2.6 Sampling and analytical procedures

Samples of the acid and base solutions were collected every two hours during stable conditions, while a higher frequency of sampling, in the range of 30-60 minutes, was used when several steady-state conditions were evaluated. During the test, flowrates, pressures, conductivities, temperature, and pH values were continuously recorded for each solution. Free chlorine in the ERS was measured employing N,N-diethyl-p-phenylenediamine colorimetric analysis.

The artificial brine was prepared mixing reverse osmosis (RO) permeate (~ 350 μS cm^{-1}) and high-grade NaCl (>99.5% purity, Saline di Volterra S.r.l.), reaching a conductivity almost equal to 67 mS cm^{-1} (i.e, the conductivity of real brine at ambient temperature).

Titrations were performed with standard solutions of 0.1 mol L^{-1} HCl for the alkaline sample and of 0.05 mol L^{-1} Na_2CO_3 for the acid one, using 10 wt.% methyl orange solution (ACS dye content 85 wt.%, SIGMA-ALDRICH) as pH indicator. Sample analysis was completed by ion chromatography (Metrohm 882 compact IC plus) to measure cations and anions concentrations, using the cation (Metrosep C 4 – 250/4.0) and anion (Metrosep A Supp 5 – 250/4.0) columns, respectively. A 5.5 mmol L^{-1} H_3PO_4 solution for the cation and a mixture of 3.2 mmol L^{-1} Na_2CO_3 and 1.0 mmol L^{-1} $NaHCO_3$ for the anion were used as eluents for the two columns, respectively.

2.7 Performance indicators and multi-ionic transport parameters

2.7.1 EDBM KPIs

The performance indicators presented in this section refer to either to the "produced NaOH" or the "produced HCl", thus assuming that the all the OH^- in the base and the H^+ in the acid were associated with the Na^+ and Cl^- ions, respectively. This assumption, already used in [35] when dealing with multi-ionic solutions, was considered reasonable for this study because of the low concentration of K^+ and SO_4^{2-} compared to Na^+ and Cl^-in the saline solutions (see Table 1).

Specific Energy Consumption (SEC) is a measure of the energy consumed to produce either 1 kg of NaOH in the alkaline solution or 1 kg of HCl in the acidic one. It is evaluated as follows:

$$SEC = \frac{U_{ex}\ i\ 2\ A_m}{60\ (Q_{sol,out}\ C_{sol,out} - Q_{sol,in}\ C_{sol,in})\ M_w} \quad [kWh\ kg^{-1}] \tag{1}$$

where i (A m^{-2}) and U_{ex} (V) are the applied current density and the corresponding stack voltage, respectively; the factor *2* accounts for the two cell packs installed in the stack; A_m represents the active membrane area of one cell pack; $Q_{sol,out}$ (L min^{-1}) and $Q_{sol,in}$ (L min^{-1}) are either the acid or alkaline flowrates at the outlet and inlet of the feed and bleed configuration, respectively. Similarly, $C_{sol,out}$ (mol L^{-1}) and $C_{sol,in}$ (mol L^{-1}) are either the acid or alkaline concentrations at the outlet and inlet of EDBM unit. It is important to note that the inlet solution was the RO permeate, thus the inlet acid/base concentration to the system was considered zero. M_w (g mol^{-1}) is either the HCl or NaOH molecular weight.

Current efficiency (CE) represents the fraction of total electric current converted in either OH^- or H^+ in the alkaline or acidic compartment, respectively. CE is defined as:

$$CE = \frac{(Q_{sol,out}\ C_{sol,out} - Q_{sol,in}\ C_{sol,in})\ z\ F}{60\ N_{tr}\ i\ A_m} 100 \quad [\%] \tag{2}$$

where z (–) is the ion valence, F (96,485 C mol^{-1}) is the Faraday constant and N_{tr} (–) is total the number of triplets installed in the stack (in both cell packs).

Specific Productivity (SP) is the measure of the amount of either NaOH or HCl produced in one working year (here assumed as 8,000 h) by the unit membrane area of the EDBM unit. SP is calculated as:

$$SP = \frac{\left(Q_{sol,out}\ C_{sol,out} - Q_{sol,in}\ C_{sol,in}\right)\ M_w\ 8000\ 60}{3\ A_m\ N_{tr}\ 10^6}\ [ton\ y^{-1}m^{-2}] \tag{3}$$

where 3 is the number of membranes per triplet.

2.7.2 Ion transport in multi-ionic systems

The presence of real solutions, containing more ions, raises the need to analyse the ions transport across the membranes of the EDBM units. Similarly to a previous work [35], the transport of ions, different than protons and hydroxides, was assumed through the monopolar CEM or AEM, thus exiting from the salt compartment and entering in the acid/base channel (as shown in Figure 3). The transport of these ions through the bipolar membrane was assumed negligible since the BM has two layers differently charged and promotes the water dissociation into protons and hydroxide ions [19]. Indeed, the limiting current related to the transport of these ions from BM interlayer to the acid/base compartments is so small that such transport can be reasonably neglected under the adopted operating conditions [41].

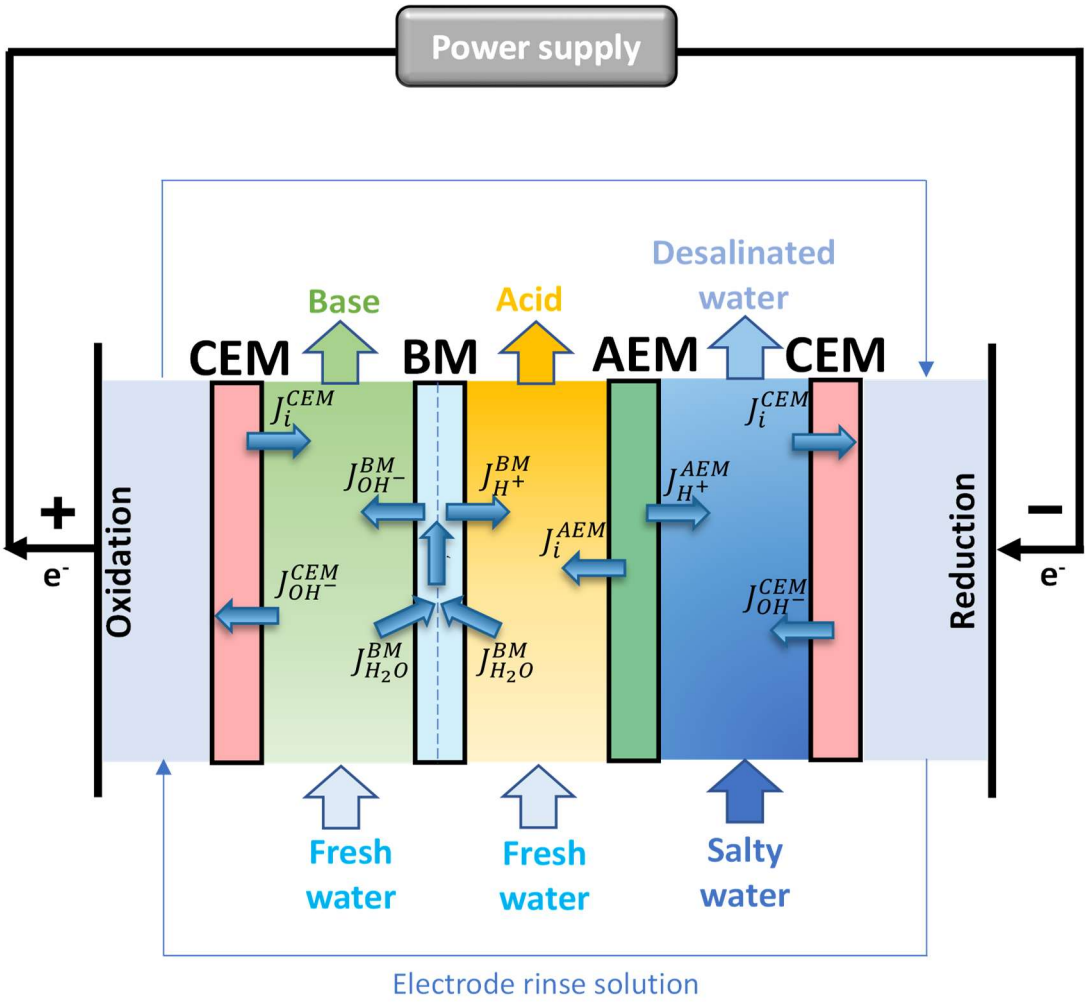

Figure 3. Simplified representation of the EDBM triplet including the main ion fluxes and the expected directions. The subscript *i* indicates the generic transported ion different from protons and hydroxides ions.

The fluxes of ions *i* different than protons and hydroxide ions, J_i^{CEM} and J_i^{AEM}, transported from the saline solution to the base/acid, across the monopolar CEM and AEM, respectively, are calculated as follows:

$$J_i^{CEM} = \frac{(Q_{base,out}\ C_{i,base,out} - Q_{base,in}\ C_{i,base,in})}{60\ A_m\ N_{tr}}\ [mol\ m^{-2}s^{-1}] \quad (4)$$

$$J_i^{AEM} = \frac{(Q_{acid,out}\ C_{i,acid,out} - Q_{acid,in}\ C_{i,acid,in})}{60\ A_m\ N_{tr}}\ [mol\ m^{-2}s^{-1}] \quad (5)$$

The fluxes, as calculated in this work, represent the net apparent fluxes, including both migration and diffusion transport phenomena.

However, monopolar membranes are also crossed by part of the OH^- and H^+ which are generated at the bipolar membrane interlayer. Indeed, the fluxes of OH^- and H^+ towards CEM and AEM, $J_{OH^-}^{CEM}$ and

$J_{H^+}^{AEM}$, respectively, can be attributed to undesirable phenomena, such as the non-ideal ion-exchange membranes (IEMs) permselectivities and the partial ion-back-diffusion, resulting in a partial neutralization and pH variation in the salt channel. These fluxes are calculated as the difference between the fluxes of the hydroxide ions and protons generated at the bipolar membrane, $J_{OH^-}^{BM}$ and $J_{H^+}^{BM}$, respectively, and the fluxes of the two ions calculated from the experimentally measured concentration in the base and acid channels. Thus, $J_{OH^-}^{CEM}$ and $J_{H^+}^{AEM}$ are calculated as:

$$J_{OH^-}^{CEM} = J_{OH^-}^{BM} - \frac{(Q_{base,out}\, C_{OH^-,base,out} - Q_{base,in}\, C_{OH^-,base,in})}{60\, A_m\, N_{tr}} \ [mol\, m^{-2} s^{-1}] \quad (6)$$

$$J_{H^+}^{AEM} = J_{H^+}^{BM} - \frac{(Q_{acid,out}\, C_{H^+,acid,out} - Q_{acid,in}\, C_{H^+,acid,in})}{60\, A_m\, N_{tr}} \ [mol\, m^{-2} s^{-1}] \quad (7)$$

where $J_{OH^-}^{BM}$ and $J_{H^+}^{BM}$, are estimated as:

$$J_{OH^-}^{BM} = J_{H^+}^{BM} = \frac{2\, i}{F} \ [mol\, m^{-2} s^{-1}] \quad (8)$$

where the factor 2 accounts for two cell-packs installed in the EDBM stack and transport numbers equal to one are assumed. Specifically, this assumption, although can be considered simplistic, is reasonable since a low parasitic current through manifolds is expected [38].

Considering the previous assumptions, the overall fluxes of ions across CEM and AEM, J_{tot}^{CEM} and J_{tot}^{AEM}, are obtained as:

$$J_{tot}^{CEM} = \sum_i J_i^{CEM} + J_{OH^-}^{CEM} \ [mol\, m^{-2} s^{-1}] \quad (9)$$

$$J_{tot}^{AEM} = \sum_i J_i^{AEM} + J_{H^+}^{AEM} \ [mol\, m^{-2} s^{-1}] \quad (10)$$

where the subscript *i* refers to K^+, Na^+, Cl^- and SO_4^{2-} ions present in the salt solution.

The apparent transport number, $t_{i,IEM}$, is thus calculated for each ion *i* across the CEM and AEM as:

$$t_{i,IEM} = \frac{J_i^{IEM}}{J_{tot}^{IEM}} \ [-] \quad (11)$$

where J_i^{IEM} and J_{tot}^{IEM} are the specific single ion and total fluxes across the generic IEM, respectively.

The apparent ion selectivity for the generic ion *i* and monopolar IEM, $Sel_{i/ref,IEM}$, is defined as the ratio between the flux of the generic ion *i* and the reference ion, *ref*, and the ratio between their concentrations in the salt compartment, as follows:

$$Sel_{i/ref,IEM} = \frac{J_i^{IEM} / J_{ref}^{IEM}}{C_{i,salt,in} / C_{ref,salt,in}} \ [-] \tag{12}$$

where $C_{i,salt,in}$ (mol L^{-1}) and $C_{ref,salt,in}$ (mol L^{-1}) are the concentrations of the generic ion, *i*, and the reference ion, *ref*, in the salt solution entering the EDBM feed and bleed configuration. Reference ions were selected as sodium and chlorides for CEM and AEM membranes, respectively.

Acid and alkaline streams composition is also evaluated calculating anionic and cationic purity, defined as follows:

$$P_{H^+,acid} = \frac{C_{H^+,acid,out}}{C_{H^+,acid,out} + C_{Na^+,acid,out} + C_{K^+,acid,out}} 100 \ [\%] \tag{13}$$

$$P_{Cl^-,acid} = \frac{C_{Cl^-,acid,out}}{C_{Cl^-,acid,out} + C_{SO_4{}^{2-},acid,out}} 100 \ [\%] \tag{14}$$

$$P_{Na^+,base} = \frac{C_{Na^+,base,out}}{C_{Na^+,base,out} + C_{K^+,base,out}} 100 \ [\%] \tag{15}$$

$$P_{OH^-,base} = \frac{C_{OH^-,base,out}}{C_{OH^-,base,out} + C_{Cl^-,base,out} + C_{SO_4{}^{2-},base,out}} 100 \ [\%] \tag{16}$$

For anions purity is possible to consider the valance of different ions through the computing of speciation, defined as:

$$S_{Cl^-,acid} = \frac{C_{Cl^-,acid,out} \ z_{Cl^-}}{C_{Cl^-,acid,out} \ z_{Cl^-} + C_{SO_4{}^{2-},acid,out} \ z_{SO_4{}^{2-}}} 100 \ [\%] \tag{17}$$

$$S_{OH^-,base} = \frac{C_{OH^-,base,out} \ z_{OH^-}}{C_{OH^-,base,out} \ z_{OH^-} + C_{Cl^-,base,out} \ z_{Cl^-} + C_{SO_4{}^{2-},base,out} \ z_{SO_4{}^{2-}}} 100 \ [\%] \tag{18}$$

where z_i is the valence of ion *i*.

3 Result and Discussion

3.1 Flowrate control strategy

The EDBM pilot was operated under flowrate control strategy for the first 32 hours, employing both artificial and real brine. For this control strategy, the performance achieved with the two brines were compared. Moreover, several steady-state conditions were evaluated while employing the real brine, by letting both the current density and solutions outlet flowrates to vary. In this way, the system behaviour was assessed in a wide range of operating conditions.

3.1.1 Comparison between artificial and real solutions

The comparison between the artificial and the real multi-ionic brine was made for a given conductivity (~ 67 mS cm^{-1} at 20 °C) of the inlet salt solutions to the EDBM unit. The operating conditions were maintained constant, keeping an outlet flowrate of acid, base and salt equal to 1.0, 0.70 and 1.8 L min^{-1}, respectively, and applying a fixed current density of 400 A m^{-2} (code 1–0.7–1.8–400).

In Figure 4, the comparison is shown in terms of KPIs, outlet concentration and measured external voltage for both acid and base product. The main differences in the transition from synthetic to real brine lie in an increase in the external voltage U_{ex} and, consequently, in the specific energy consumption for both chemicals. For the alkaline product, an increase of 3 % was observed in the current efficiency, specific productivity, and concentration, with values of 49 % of CE, 0.8 ton y^{-1} m^{-2} of SP and 1.1 mol L^{-1} of concentration, respectively. Regarding the SEC, an increase from 3.5 kWh kg^{-1} to 4.0 kWh kg^{-1} was noted for the base product. For the acid, conversely, a reduction of about 10 % in CE, SP and concentration was measured, with values of 35 % of CE, 0.52 ton y^{-1} m^{-2} of SP and 0.56 mol L^{-1} of concentration, respectively. Also in this case, the SEC showed an increase passing from 4.7 kWh kg^{-1} to 6.2 kWh kg^{-1}, moving from artificial to real brine.

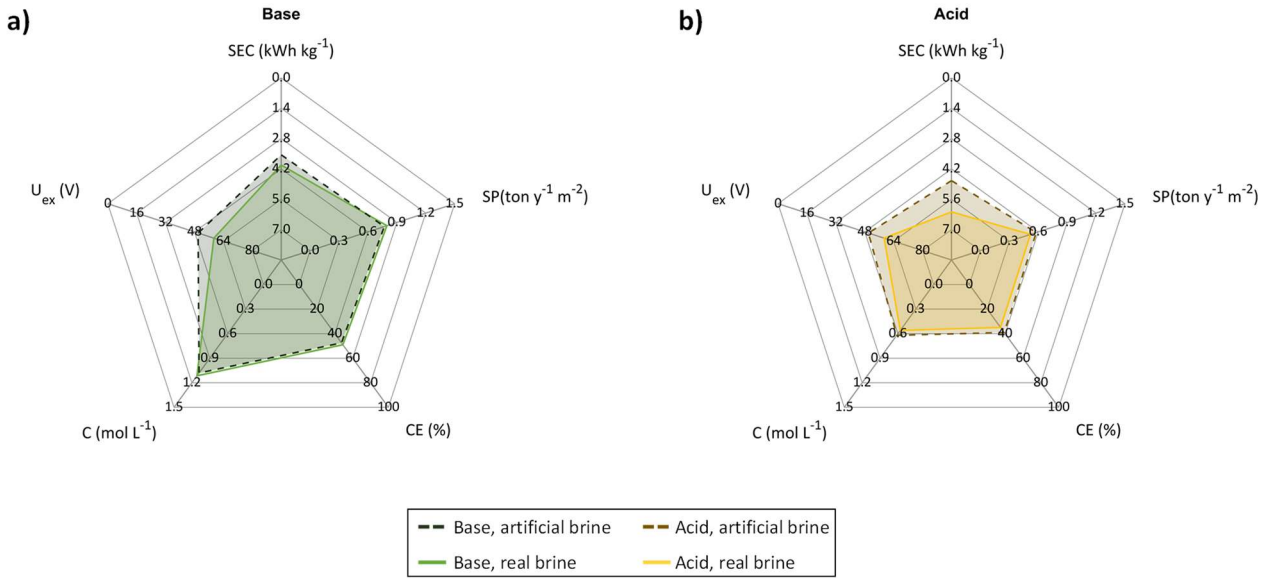

Figure 4. Spider-plots highlighting the main differences in EDBM performance when an artificial and a real salt solution are adopted, under flowrate control mode. KPIs, concentration and measured external voltage are shown for both produced chemicals. Operating condition 1–0.7–1.8–400 (i.e., acid flowrate–base flowrate–salt flowrate–current density) was used. The comparison was made at equal conductivity of the inlet salt solutions (~ 67 mS cm^{-1} at 20 °C).

The utilisation of the real brine had a beneficial effect on the alkaline product, for which the performance parameters such as CE and SP as well as the outlet concentration increased. Conversely, the SEC was mainly affected by the voltage and an increase was also observed. In general, the performance improvement could be attributed to the presence of hydroxide ions in the brine (pH of around 13). Looking at the acid product, the use of the real salt solution led to a performance reduction. Indeed, the acid channel received hydroxide ions that neutralized the produced acid, leading to a concentration reduction. This undesired effect can be tolerated since the alkaline product represents the most valuable chemical [22]. In Figure S2a, the pH of the inlet and outlet salt solution are shown as function of time, straddling the transition from artificial to real salt solution. All the illustrated points represent samples collected in steady-state conditions. It could be observed as the salt compartment reduced his pH in both cases, compared to the inlet pH value. When an artificial solution was employed, the pH of the salt stream went from an almost neutral pH to a value close to 2. Conversely, when the real brine was adopted, the pH decreased from 13 to 9. The acidification of the salt solution is in general an undesired phenomena, but in this case it has a double beneficial

effect: i) it improves the performance indicator (i.e., CE and SP) and the concentration of the base streams; ii) it reduces the outlet salt stream pH to a value closer to the neutrality so that it can be sent to the downstream processes (evaporative pounds) without any further treatment (i.e., pH correction). On the other side, the increase in external voltage can be attributed to the smaller salt content of the real brine. Indeed, the comparison was made keeping the conductivity of the inlet salt stream constant, but different values of outlet conductivity were reached. This is related to the lower salt content of the real brine, which passe though the same stack, at fixed operating conditions, led to a lower outlet conductivity of the real brine, FigureS2b. This reduction in the outlet salt concentration, produced an increase in the external voltage, as already observed in a previous work [42].

3.1.2 Comparison between different set of operating conditions

Following the comparison between real and artificial solutions, the flowrate control strategy was further studied evaluating different sets of operative conditions to assess the behaviour of the system when a real brine is employed. The comparison of these scenarios is reported in Figure 5

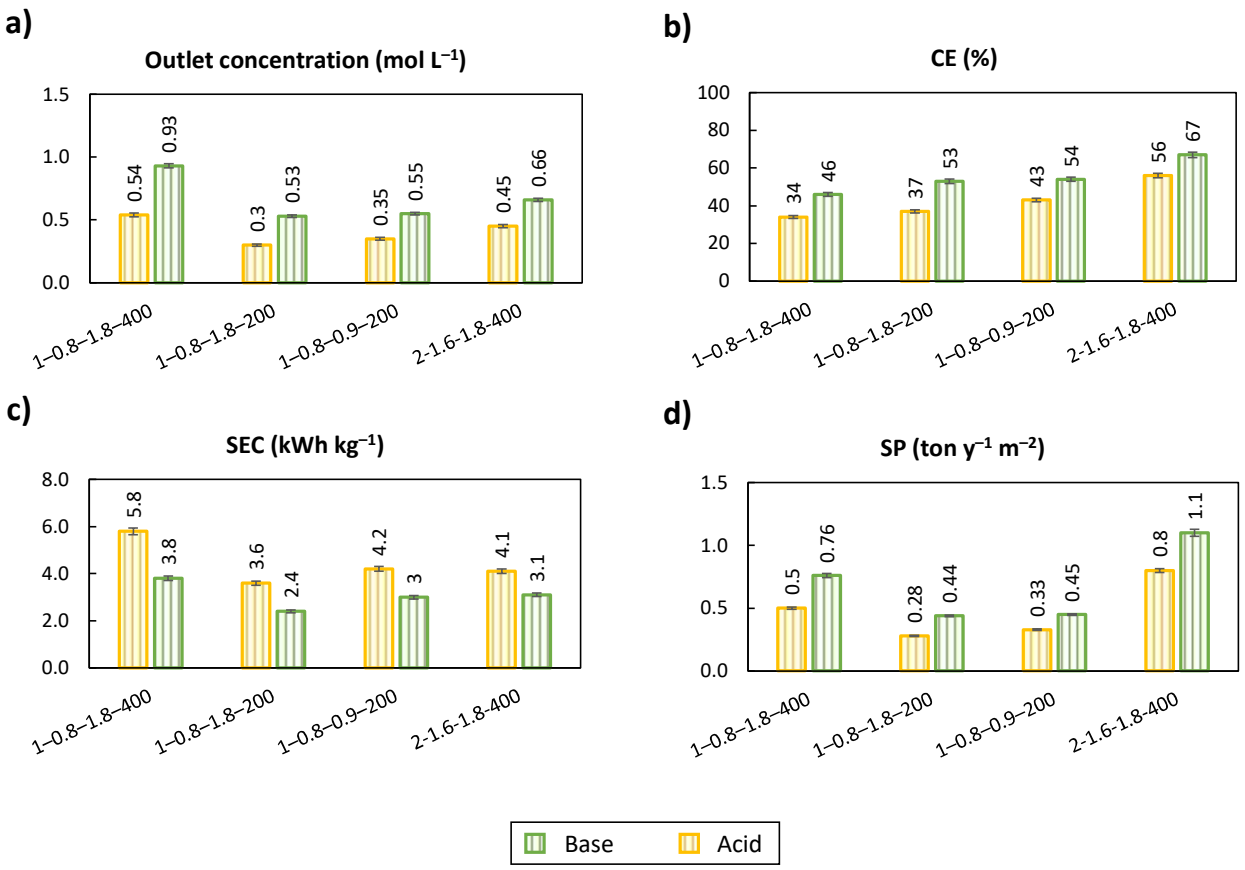

Figure 5. Values of chemicals concentration and key performance parameters recorded in four different operating conditions under flowrate control mode, employing the real salt solution. The operating conditions are reported with the following coding: acid flowrate (L min^{-1}) – base flowrate (L min^{-1}) – salt flowrate (L min^{-1}) – current density (A m^{-2}).

In the first evaluated set of operating conditions, acid, base, and salt outlet flowrate of 1, 0.8, and 1.8 L min^{-1}, respectively were used, and a current density of 400 A m^{-2} was applied to the EDBM stack (i.e., operating condition 1–0.8–1.8–400). Under these operating conditions, values of concentration of 0.54 mol L^{-1} and 0.93 mol L^{-1} for acid and base, respectively were obtained, (Figure 5). The corresponding current efficiency resulted quite low, and the SEC reached a value of 5.8 kWh kg^{-1} and 3.8 kWh kg^{-1} for acid and base, respectively. In the second conditions, halving the current density (i.e., 1–0.8–1.8–200), lower concentrations were obtained (of 0.3 mol L^{-1} and 0.53 mol L^{-1} for acid and base, respectively). This resulted in an improvement of the system performance in terms of SEC and CE, with value for the alkaline product of 2.4 kWh kg^{-1} and 53%, respectively. Conversely, a significant reduction in the SP was observed due to his proportionality to the current density and

current efficiency, with absolute values of 0.28 ton y^{-1} m^{-2} and 0.44 ton y^{-1} m^{-2} for acid and base, respectively. In the third operating condition, reducing by half also the outlet salt flowrate (i.e., 1–0.8–0.9–200) an increase of the acid concentrations was observed, while the base concentration remained unchanged compared to second case. The concentration increase in the acid line might be attributed to a passage of hydroxide ions from the salt to the acid chamber, being reduced by the lower salt flowrate. In the fourth case, doubling all flowrates and the current density (i.e., 2–1.6–1.8–400) produced an increase of chemicals concentration to values of 0.45 mol L^{-1} and 0.66 mol L^{-1} for acid and base, respectively. Interestingly, the obtained concentration resulted significant lower compared to first scenario (i.e., 1–0.8–1.8–400), leading to higher performance, with values of CE between 54 % and 67 % as well as value of SP 0.8 ton y^{-1} m^{-2} and 1.1 ton y^{-1} m^{-2}, for acid and base, respectively. These results confirmed that the feed and bleed configuration shows better performance once the current density is increased and the outlet chemicals concentration are reduced, as reported also in [29,38].

Lastly, the effect of increasing salt/acid and salt/base outlet flowrate ratio was investigated at high current density (i.e., 400 Am^{-2}). Specifically, starting from operating condition 2–1.6–1.8–400, the outlet salt flowrate was increased of 0.5 L min^{-1} (i.e., up to 2.3 L min^{-1}) and its effect on chemicals concentration and KPIs was evaluated. For sake of brevity these results are reported in the supplementary material (Figure S3), and show how outlet acid and base concentration result almost unchanged, while a significant reduction in the SEC (by 20%) was recorded. This effect was related to the higher outlet salt conductivity, which passed from 5 mS cm^{-1} to 17 mS cm^{-1}, leading to a voltage reduction from 62.5 V to 53 V.

3.2 Pressure control strategy

The EDBM pilot was operated under pressure control strategy for 27 hours, testing both artificial and real brine. Several operating conditions were evaluated employing the real brine, to investigate the performance of the system in a wide range of operating conditions. In addition, a comparison between

the two control strategies was made at fixed operating condition, using the real salt solution. Finally, artificial and real solution were compared under similar operating condition.

3.2.1 Comparison between different set of operating conditions

Several scenarios were investigated under pressure control strategy by letting operating conditions to vary. The same values of current density (i.e., 400 A m^{-2} and 200 A m^{-2}) and salt outlet flowrate (i.e., 1.8 L min^{-1} and 2.3 L min^{-1}) as in the flowrate control case were evaluated. On the other hand, higher values of acid and base outlet flowrates were considered in order to compare the system performance under similar values of outlet chemicals concentration (due to the better performance achieved). The comparison between different set of operating conditions in terms of outlet concentration and KPIs is presented in Figure 6. In the first evaluated set of operating conditions (code 1.4–1.1–1.8–400) values of concentration of 0.65 mol L^{-1} and 1.03 mol L^{-1} for acid and base, respectively were obtained. Improved performance indicators were obtained, with values of 71% % of CE, 1.2 ton y^{-1} m^{-2} of SP and 2.6 kWh kg^{-1} of SEC for alkaline product.

Comparing sets of operating condition 1.4–1.1–1.8–400 and 1.4–1.1–1.8–200, a reduction in concentration, SEC and SP in the range 40–43 % was observed for both products in the second case. Whilst an improvement in the CE of about 18 % was registered for acid and base. Interestingly, for the base stream absolute values of 84 % of CE, 1.5 kWh kg^{-1} of SEC were obtained at 0.62 mol L^{-1} of concentration. This performance appears promising, considering the size of the unit (i.e., semi-industrial scale) and the employment of a real brine with a reduced salt content (Table 1). Decreasing the flowrate of both chemicals (i.e., 1.2–1–1.8–400) produced an increase in concentration to values of 0.77 mol L^{-1} and 1.1 mol L^{-1} for acid and base, respectively. Interestingly, the SEC showed a reduction of 8–19 % for both chemicals. This effect was mainly related to the voltage reduction which was, in turn, produced by the conductivity increase in the outlet brine (i.e., lower conversion of salt). Increasing the outlet flowrate of the acid stream of 0.1 L min^{-1} (i.e., operating condition 1.5–1.1–1.8–400) compared to operating condition 1.4–1.1–1.8–400, allowed to study the potential interaction

between products. Specifically, it was possible to see whether a reduction in outlet acid concentration can have a positive effect on the base product (i.e., the pH gradient between the compartments is reduced). However, no improvements were observed for the base product, suggesting that diffusive processes did not have a high impact.

Furthermore, also for this control strategy the effect of increasing the outlet flowrate of the salt streams of + 0.5 L min^{-1} was evaluated in terms of outlet concentration and KPIs are reported in the supplementary material for the sake of brevity (Figure S4). An increase in the performance was observed, especially for the base streams. The most meaningful effect was the SEC reduction (5–24 %) due to the higher conductivity of the outlet salt stream. These results suggested that the higher availability of the real brine has a beneficial effect on EDBM performance of the base product, while maintaining similar KPIs and concentration for the acid one.

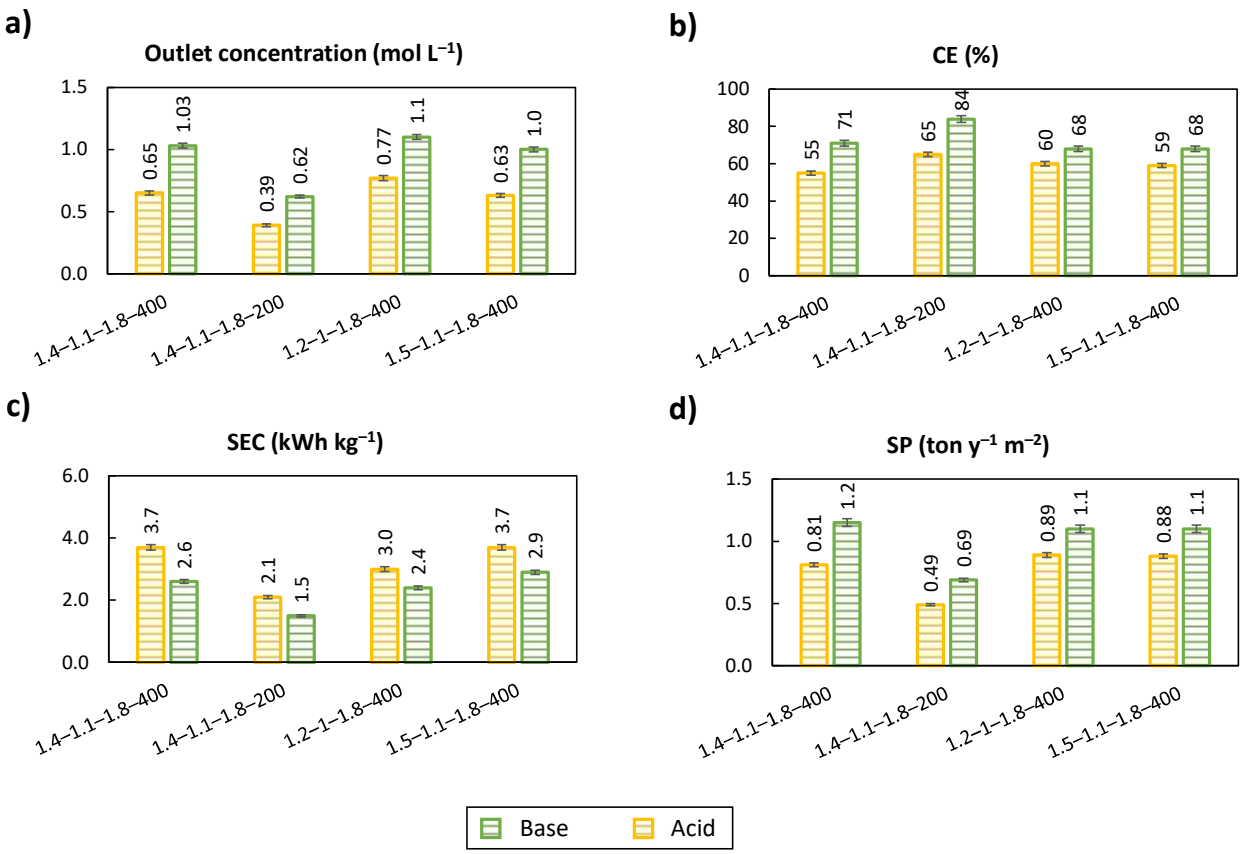

Figure 6. Four different performance parameters as a function of different operating conditions under pressure control mode, employing a real salt solution. In the X axis the operating conditions of the EDBM unit are reported in the following form: acid flowrate (L min^{-1}) – base flowrate (L min^{-1}) – salt flowrate (L min^{-1}) – current density (A m^{-2}).

3.2.2 Comparison between flowrate and pressure control strategies

Following the observation of better performance under pressure control strategy, a quantitative analysis is here reported. The same operating condition was evaluated utilizing the real brine. In Figure 7, the comparison between the control strategies is presented in terms of outlet concentration, external voltage and KPIs. A significant performance improvement was observed moving from flowrate to pressure control. More in detail, improvements in outlet concentration and KPIs in the range 32–43 % were observed, for both acid and base. For the base stream, a CE of 63 % and a SEC of 2.6 kWh kg^{-1} were obtained at a concentration of 1.3 mol L^{-1} under pressure control. This significant improvement in the performance was mainly related to the reduction of convective fluxes through the membranes between adjacent compartments, generated from the different pressure

distributions. Although, the same geometry of the compartments (i.e., acid, base and salt) and the same volume flowrates were used, during several hours of operations meaningful difference in the pressure losses can be found. This effect is allegedly generated by deformation processes for membranes and spacers and possible fouling phenomena. Indeed, inlet pressures of the compartment were monitored under flowrate control strategy and average values of 1.0 barg, 1.5 barg and 1.1 barg for acid, base and salt, respectively, were found during the test under flowrate control strategy.

In terms of purity, acid products quality improved significatively, passing from a cationic purity of 50% to 85%. Instead the anionic purity of the acid product remained quite high passing from 95% to 90 % (from 90% to 80% in terms of speciation). Almost constant purity were observed for alkaline product in the both control mode, with values higher than 95% for both cationic and anionic purity. Employing the pressure control strategy allowed this undesired effect to be tackled, thus guaranteeing high performance of the EDBM.

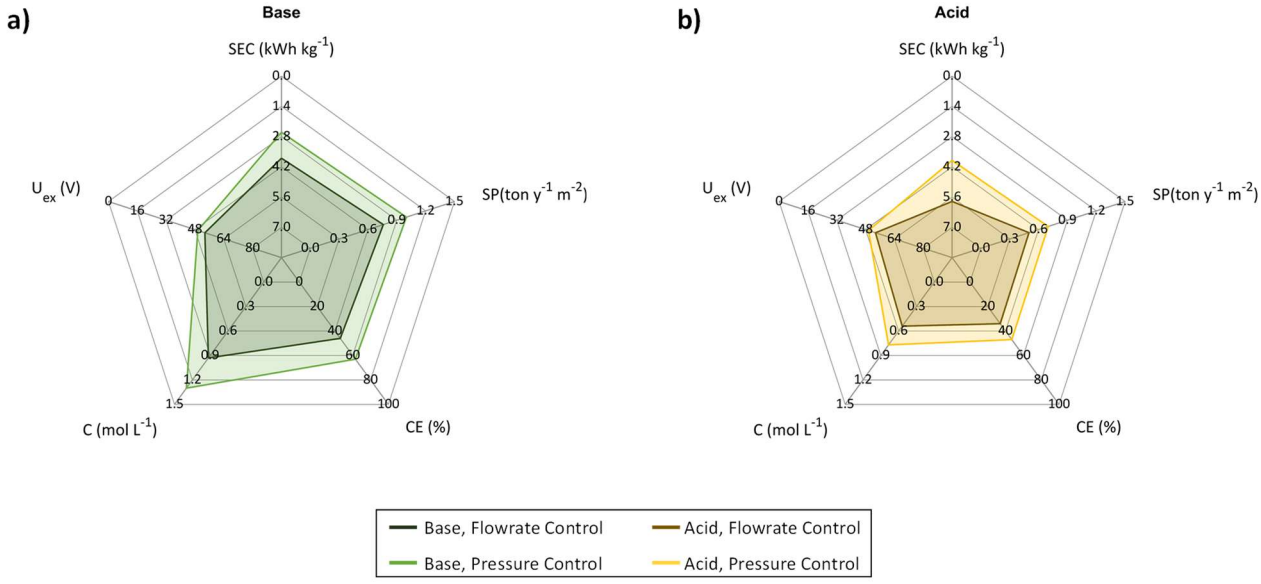

Figure 7. Comparison in terms of KPIs, concentration and external voltage between flowrate and pressure control strategies at fixed operating condition (i.e., 1–0.8–1.8–400), employing the real brine.

3.2.3 Comparison between artificial and real solutions

The effect of utilising artificial and real brine was also evaluated for the pressure control strategy and the results are shown in Figure 8. For the alkaline product an improvement of all the KPIs was observed at constant concentration of 1.3 mol L^{-1}, reaching values of 2.6 kWh kg^{-1}, 63 % and 1 ton y^{-1} m^{-2} for SEC, CE and SP, respectively, in the case of real brine. On the other hand, the acid product was negatively affected by pH of the real brine, leading to a slight reduction in concentration and KPIs, with variation in the range of 6-10 %. These results differ from what obtained under flowrate control strategy, where the major effect was an increase in the voltage passing to from artificial to real solution. Under pressure control mode, the voltage remained unchanged due to the outlet brine conductivity which was higher than 15 mS^{-1}.

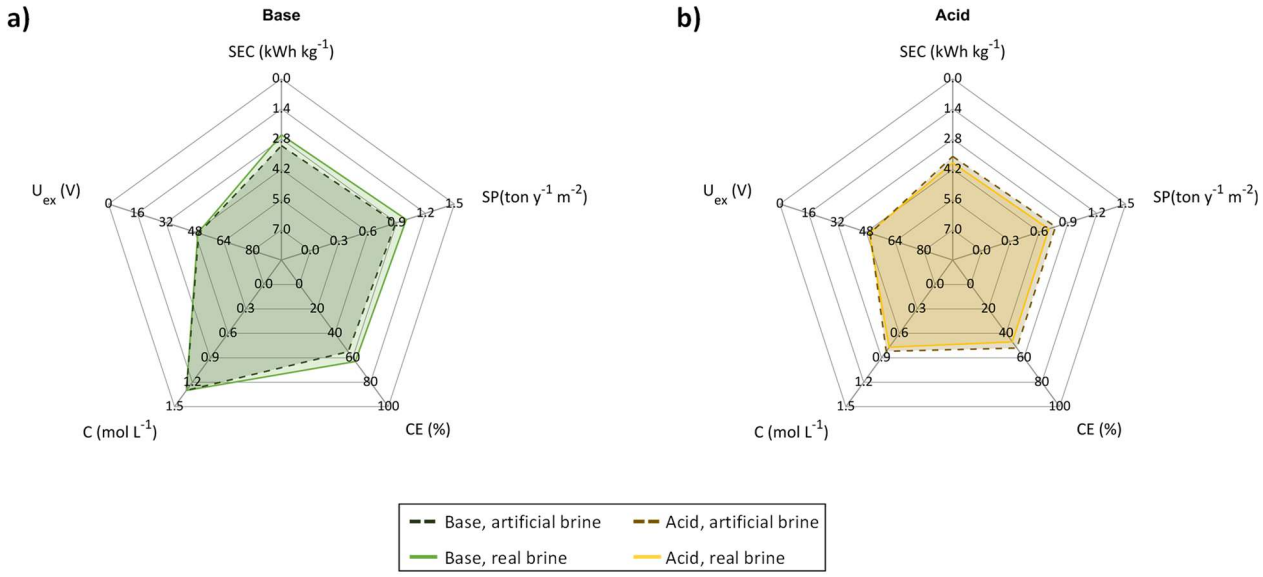

Figure 8. Comparison in terms of KPIs, concentration and external voltage between artificial (i.e., 1–0.7–1.8–400) and real brine (i.e., 1–0.8–1.8–400), under pressure control mode.

3.3 Ion transport analysis

To further assess the pilot operation with real salt solution, an analysis of ions transport across membranes was conducted. Apparent transport numbers and selectivity of each ion in IEMs were calculated from concentrations and flowrates of inlet and outlet streams (see Section 2.7.2). This

analysis is here reported only for the phase 3 of the test, in which the pressure control strategy and real brine were used. Indeed, convective fluxes observed under flowrate control mode (phases 1 and 2 of the test), related to internal passage of solution from one compartment to the adjacent ones through the membranes, would dramatically reduce the reliability of present results. The results of the analysis are depicted in Figure 9.

For anion exchange membrane (AEM) similar values of apparent transport number were observed for Cl^- and H^+, ranging at 400 A m^{-2} from 0.36 to 0.5, depending on the operating conditions. It should be noted that the transport of these ions takes place in opposite directions: Cl^- ions move from the salt to the acid compartment while H^+ ions go from the acid to the salt compartment. Therefore, a considerable quantity of protons was lost in the salt channel, thus reducing the CE of the acid product. When the current density was halved, the transport number of protons was reduced, reaching a value of 0.3, while the one of Cl^- increased to 0.55. This effect was mainly due to protons generation reduction in the BM, which led to a lower concentration of protons in the acid chamber. The other ions (i.e, Na^+, K^+ and SO_4^{2-}) exhibited very low transport numbers with values lower than 0.1. This was expected due to their ion charge, in the case of cations, and the reduced concentration of SO_4^{2-} [35]. Looking at the selectivity of the AEM, which employed Cl^- as a reference ion, a value around 1 was obtained also for the SO_4^{2-}, whilst a reduced selectivity, lower than 0.2, was found for the cations. Analysing the CEM behaviour, high values of Na^+ transport number in range 0.6–0.8 were observed. Hydroxide ions showed a transport number close to 0.3 at 400 Am^{-2} and it was almost halved at 200 A m^{-2}. This was confirmed by higher values of CE found at 200 A m^{-2} (i.e., 84%). For the other ions (i.e., Cl^-, SO_4^{2-}, K^+), values lower than 0.05 were observed. Regarding the apparent selectivity of the CEM, similar values were observed between Na^+ and K^+, while for other ions it appeared negligible being lower than 0.1.

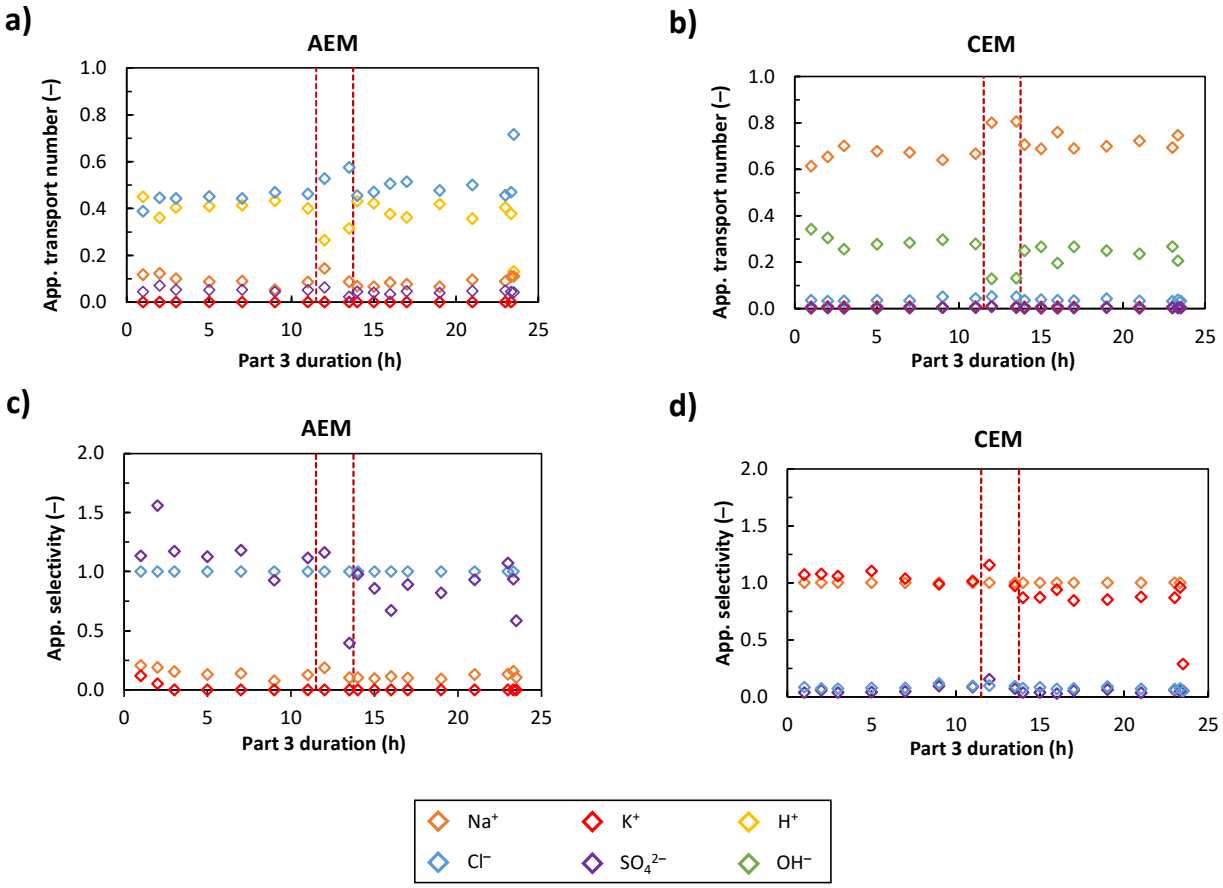

Figure 9. Apparent transport numbers and selectivity profiles versus time under pressure control strategy and employing a real brine. Red dashed lines delimit the region in which the current density was halved from the initial value of 400 A m^{-2}, to the final one of 200 A m^{-2}. AEM= anion exchange membrane, CEM= cation exchange membrane.

4 Conclusions

This work presented for the first time a comprehensive analysis of the performance of a large scale EDBM unit operated in continuous mode, with artificial and real brines. The risk mitigation strategies taken to ensure safe operation of the system were described in detail. Two different control strategies were evaluated in a single operational run of 59 h: i) flowrate and ii) pressure control strategy. The performance of the system with artificial and real brines was compared for both control strategies. Under flowrate control, the main effect observed was an increase of the SEC (in the range14-30 %) when the real brine was employed, while an improvement and a slight reduction of the performance was observed in the alkaline and acid products, respectively, under pressure control mode. With the flowrate control strategy the best results were obtained adopting the set of operating conditions 2–

1.6–1.8–400 (i.e., acid flowrate (L min^{-1}) – base flowrate (L min^{-1}) – salt flowrate (L min^{-1}) – current density (A m^{-2}), respectively) , with values of 67% of CE, 3.1 kWh kg^{-1} of SEC, 1.1 ton y^{-1} m^{-2} of SP for a base product concentration of 0.66 mol L^{-1}. Adopting the pressure control strategy, the best KPIs were achieved adopting the set of operating conditions 1.4–1.1–1.8–200, due to the lower alkaline concentration reached of 0.62 mol L^{-1}, with values of 84% of CE, 1.5 kWh kg^{-1} of SEC, 0.7 ton y^{-1} m^{-2} of SP. Flowrate and pressure control strategy were compared employing real brine, showing significant improvements in concentration and KPIs up to 40% (i.e., set of operating conditions 1–0.8–1.8–400) were registered. This effect was related to the minimization of convective fluxes between compartments through the membranes, that arise from the different pressure distribution within the compartments under flowrate control strategy. Finally, an in-depth study of the ions transport in pressure control was conducted, evaluating apparent transport number and selectivity. In the AEM comparable values of transport number were observed for Cl^{-1} and H^{+}, while in the CEM a significant higher value was observed for Na^{+} compared to OH^{-1}. Regarding the apparent selectivity of the membranes, similar values were observed for Cl^{-1} and SO_4^{2-} in the AEM, as well as for Na^{+} and K^{+} in the CEM. Moreover, in all the cases, anionic purity of the acid product and cationic purity of the alkaline product above 90 % were obtained.

These results highlighted the adaptability of EDBM process to real industrial scenarios, of waste brine valorisation, showcasing the technology potential with MLD and ZDL treatment chain for the recovery of high value-added materials.

Author Statement

Giovanni Virruso[†]: writing – original draft, visualization, formal analysis, investigation, methodology, data curation, software

Calogero Cassaro[†]: writing – original draft, visualization, formal analysis, investigation, methodology, data curation, software

Fabrizio Vassallo: writing – original draft, investigation, formal analysis, supervision

Antonia Filingeri: writing – original draft, investigation, formal analysis

Alessandra Pellegrino: writing – original draft, investigation, formal analysis

Alessandro Tamburini: Methodology, Validation, Resources, Writing – review & editing, Supervision, Project administration, Funding acquisition.

Andrea Cipollina: Conceptualization, Methodology, Validation, Resources, Writing – review & editing, Supervision, Project administration, Funding acquisition.

Giorgio Micale: Conceptualization, Methodology, Validation, Resources, Writing – review & editing, Supervision, Project administration, Funding acquisition.

Acknowledgements

This project has received funding from the European Union's Horizon 2020 research and innovation program under Grant Agreement no. 869474 (WATER-MINING-next generation water-smart management systems: large scale demonstrations for a circular economy and society). www.watermining.eu.

We would like to thank FuMA-Tech GmbH (Germany) for suppling the stack and providing valuable advice and guidance during the troubleshooting activities.

Abbreviation

A	Artificial brine
AEM	Anion exchange membrane
BM	Bipolar membrane
CE	Current efficiency
CEM	Cation exchange membrane
DC	Direct current
DSA	Dimensionally stable anode
ED	Electrodialysis
EDBM	Electrodialysis with bipolar membranes
EP	Evaporative pond
ERS	Electrodes rinse solution
F	Flowrate control strategy
H2ccys	Carbocysteine
IEM	Ion-exchange membrane
IEX	Ion-exchange resins
KPI	Key performance indicators
MED	Multiple effect distillation
MF-PFR	Multiple feed plug flow reactor
MLD	Minimum liquid discharge
NF	Nanofiltration
P	Pressure control strategy
PFD	Process flow diagram
PLC	Programmable logic controller
R	Real brine
RO	Reverse osmosis
SEC	Specific energy consumption
SED	Selectrodialysis
SP	Specific productivity
UF	Ultrafiltration
ZLD	Zero liquid discharge

Symbols

A_m (m^2)	Active membrane area
M_w (C mol^{-1})	Molecular weight
N_{tr} (-)	Number of triplets
U_{ex} (V)	External voltage applied to the stack
P (%)	Purity
S (%)	Speciation
C (mol L^{-1})	Molar concentration
F (C mol^{-1})	Faraday constant
J (mol m^{-2} s^{-1})	Molar flux
Q (L min^{-1})	Volumetric flowrate
i (A m^{-2})	Current density
t (-)	Transport number
z (-)	Ion valence

Subscripts

acid	Acid stream
AEM	Anion exchange membrane
base	Base stream
BM	Bipolar membrane
CEM	Cation exchange membrane

i	Generic ion
IEM	Ion-exchange membrane
in	Inlet stream
out	Outlet stream
ref	Reference ion
salt	Salt stream
tot	total

References

[1] D. Puyol, D.J. Batstone, T. Hülsen, S. Astals, M. Peces, J.O. Krömer, Resource recovery from wastewater by biological technologies: Opportunities, challenges, and prospects, Front Microbiol 7 (2017). https://doi.org/10.3389/fmicb.2016.02106.

[2] European Parliament, Water protection and management, (n.d.). https://www.europarl.europa.eu/factsheets/en/sheet/74/water-protection-and-management (accessed February 5, 2024).

[3] Muhammad Yaqub, W. Lee, Zero-liquid discharge (ZLD) technology for resource recovery from wastewater: A review, Science of the Total Environment 681 (2019) 551–563. https://doi.org/10.1016/j.scitotenv.2019.05.062.

[4] T. Tong, M. Elimelech, The Global Rise of Zero Liquid Discharge for Wastewater Management: Drivers, Technologies, and Future Directions, Environ Sci Technol 50 (2016) 6846–6855. https://doi.org/10.1021/acs.est.6b01000.

[5] A. Panagopoulos, K.-J. Haralambous, Minimal Liquid Discharge (MLD) and Zero Liquid Discharge (ZLD) strategies for wastewater management and resource recovery-Analysis, challenges and prospects, J Environ Chem Eng 8 (2020). https://doi.org/10.1016/j.jece.2020.104418.

[6] A. Panagopoulos, Techno-economic assessment of zero liquid discharge (ZLD) systems for sustainable treatment, minimization and valorization of seawater brine, J Environ Manage 306 (2022) 114488. https://doi.org/10.1016/J.JENVMAN.2022.114488.

[7] A. Panagopoulos, V. Giannika, Comparative techno-economic and environmental analysis of minimal liquid discharge (MLD) and zero liquid discharge (ZLD) desalination systems for seawater brine treatment and valorization, Sustainable Energy Technologies and Assessments 53 (2022). https://doi.org/10.1016/j.seta.2022.102477.

[8] G. Cipolletta, N. Lancioni, Ç. Akyol, A.L. Eusebi, F. Fatone, Brine treatment technologies towards minimum/zero liquid discharge and resource recovery: State of the art and techno-economic assessment, J Environ Manage 300 (2021). https://doi.org/10.1016/j.jenvman.2021.113681.

[9] R.W. Baker, Membrane Technology and Applications, Second, Wiley, London, 2012. https://doi.org/10.1002/9781118359686.

[10] A. Culcasi, R. Ktori, A. Pellegrino, M. Rodriguez-Pascual, M.C.M. van Loosdrecht, A. Tamburini, A. Cipollina, D. Xevgenos, G. Micale, Towards sustainable production of minerals and chemicals through seawater brine treatment using Eutectic freeze crystallization

and Electrodialysis with bipolar membranes, J Clean Prod 368 (2022). https://doi.org/10.1016/j.jclepro.2022.133143.

[11] D.G. Randall, J. Nathoo, A.E. Lewis, A case study for treating a reverse osmosis brine using Eutectic Freeze Crystallization-Approaching a zero waste process, Desalination 266 (2011) 256–262. https://doi.org/10.1016/j.desal.2010.08.034.

[12] A. Panagopoulos, K.-J. Haralambous, M. Loizidou, Desalination brine disposal methods and treatment technologies - A review, Science of the Total Environment 693 (2019). https://doi.org/10.1016/j.scitotenv.2019.07.351.

[13] F. Vassallo, D. La Corte, N. Cancilla, A. Tamburini, M. Bevacqua, A. Cipollina, G. Micale, A pilot-plant for the selective recovery of magnesium and calcium from waste brines, Desalination 517 (2021). https://doi.org/10.1016/j.desal.2021.115231.

[14] A. Kumar, G. Naidu, H. Fukuda, F. Du, S. Vigneswaran, E. Drioli, J.H. Lienhard, Metals Recovery from Seawater Desalination Brines: Technologies, Opportunities, and Challenges, ACS Sustain Chem Eng 9 (2021) 7704–7712. https://doi.org/10.1021/acssuschemeng.1c00785.

[15] M. Lu, L. Shao, Y. Yang, P. Li, Simultaneous Recovery of Lithium and Boron from Brine by the Collaborative Adsorption of Lithium-Ion Sieves and Boron Chelating Resins, Ind Eng Chem Res 62 (2023) 1508–1522. https://doi.org/10.1021/acs.iecr.2c03650.

[16] Z. Ye, X. Yin, L. Chen, X. He, Z. Lin, C. Liu, S. Ning, X. Wang, Y. Wei, An integrated process for removal and recovery of Cr(VI) from electroplating wastewater by ion exchange and reduction–precipitation based on a silica-supported pyridine resin, J Clean Prod 236 (2019). https://doi.org/10.1016/j.jclepro.2019.117631.

[17] M. AzadiAghdam, A. Achilli, S.A. Snyder, J. Farrell, Increasing water recovery during reclamation of treated municipal wastewater using bipolar membrane electrodialysis and fluidized bed crystallization, Journal of Water Process Engineering 38 (2020). https://doi.org/10.1016/j.jwpe.2020.101555.

[18] Y. Tanaka, Ion Exchange membranes: Fundamentals and Applications, Elsevier B.V., Amsterdam, 2007.

[19] R. Pärnamäe, S. Mareev, V. Nikonenko, S. Melnikov, N. Sheldeshov, V. Zabolotskii, H.V.M. Hamelers, M. Tedesco, Bipolar membranes: A review on principles, latest developments, and applications, J Memb Sci 617 (2021). https://doi.org/10.1016/j.memsci.2020.118538.

[20] A.M. Rajesh, T. Chakrabarty, S. Prakash, V.K. Shahi, Effects of metal alkoxides on electro-assisted water dissociation across bipolar membranes, Electrochim Acta 66 (2012) 325–331. https://doi.org/10.1016/j.electacta.2012.01.102.

[21] S.S. Mel'nikov, O.V. Shapovalova, N.V. Shel'deshov, V.I. Zabolotskii, Effect of d-metal hydroxides on water dissociation in bipolar membranes, Petroleum Chemistry 51 (2011) 577–584. https://doi.org/10.1134/S0965544111070097.

[22] A. Culcasi, L. Gurreri, A. Cipollina, A. Tamburini, G. Micale, A comprehensive multi-scale model for bipolar membrane electrodialysis (BMED), Chemical Engineering Journal 437 (2022) 135317. https://doi.org/10.1016/J.CEJ.2022.135317.

[23] H. Strathmann, Ion-Exchange Membrane Separation Processes, First edit, Elsevier B.V., 2004.

[24] W.C. Hung, R.S. Horng, C.H. Tsai, Effects of process conditions on simultaneous removal and recovery of boron from boron-laden wastewater using improved bipolar membrane electrodialysis (BMED), Journal of Water Process Engineering 47 (2022). https://doi.org/10.1016/j.jwpe.2022.102650.

[25] H. Ma, S. Yue, H. Li, Q. Wang, M. Tu, Recovery of lactic acid and other organic acids from food waste ethanol fermentation stillage: Feasibility and effects of substrates, Sep Purif Technol 209 (2019) 223–228. https://doi.org/10.1016/j.seppur.2018.07.031.

[26] M. Reig, S. Casas, O. Gibert, C. Valderrama, J.L. Cortina, Integration of nanofiltration and bipolar electrodialysis for valorization of seawater desalination brines: Production of drinking and waste water treatment chemicals, Desalination 382 (2016) 13–20. https://doi.org/10.1016/j.desal.2015.12.013.

[27] S. Valluri, S.K. Kawatra, Reduced reagent regeneration energy for CO<inf>2</inf> capture with bipolar membrane electrodialysis, Fuel Processing Technology 213 (2021). https://doi.org/10.1016/j.fuproc.2020.106691.

[28] T. León, S. Abdullah Shah, J. López, A. Culcasi, L. Jofre, A. Cipollina, J.L. Cortina, A. Tamburini, G. Micale, Electrodialysis with Bipolar Membranes for the Generation of NaOH and HCl Solutions from Brines: An Inter-Laboratory Evaluation of Thin and Ultrathin Non-Woven Cloth-Based Ion-Exchange Membranes, Membranes (Basel) 12 (2022). https://doi.org/10.3390/membranes12121204.

[29] C. Cassaro, G. Virruso, A. Culcasi, A. Cipollina, A. Tamburini, G. Micale, Electrodialysis with Bipolar Membranes for the Sustainable Production of Chemicals from Seawater Brines at Pilot Plant Scale, ACS Sustain Chem Eng 11 (2023) 2989–3000. https://doi.org/10.1021/acssuschemeng.2c06636.

[30] N. Adiba, X. Wang, C. Chang, X. Xu, Y. Liu, C. Ji, Q. Wang, Y. Ren, J. Wang, Z. Liu, Z. Ma, J. Gao, Multi-stage membrane integrated system to achieving low-mixed-salt-discharge of high-salinity mining wastewater: System design and experimental validation, Chemical Engineering Research and Design 202 (2024) 12–22. https://doi.org/10.1016/j.cherd.2023.12.015.

[31] Z. Peng, H. Wang, Y. Cheng, X. Ma, Y. Chu, X. Hu, Treatment of carbocysteine wastewater by bipolar membrane electrodialysis: From lab-to pilot-scale, J Memb Sci 687 (2023). https://doi.org/10.1016/j.memsci.2023.122056.

[32] G. Jiang, H. Li, M. Xu, H. Ruan, Sustainable reverse osmosis, electrodialysis and bipolar membrane electrodialysis application for cold-rolling wastewater treatment in the steel industry, Journal of Water Process Engineering 40 (2021). https://doi.org/10.1016/j.jwpe.2021.101968.

[33] X. Zhao, X. Cheng, J. Sun, J. Liu, Z. Liu, Y. Wang, J. Pan, Zero Liquid Discharge and Resource Treatment of Low-Salinity Mineralized Wastewater Based on Combing Selectrodialysis with Bipolar Membrane Electrodialysis, Separations 10 (2023). https://doi.org/10.3390/separations10040269.

[34] M. Reig, S. Casas, C. Valderrama, O. Gibert, J.L. Cortina, Integration of monopolar and bipolar electrodialysis for valorization of seawater reverse osmosis desalination brines: Production of strong acid and base, Desalination 398 (2016) 87–97. https://doi.org/10.1016/j.desal.2016.07.024.

[35] A. Filingeri, J. Lopez, A. Culcasi, T. Leon, A. Tamburini, J. Luis Cortina, G. Micale, A. Cipollina, In-depth insights on multi-ionic transport in Electrodialysis with bipolar membrane systems, Chemical Engineering Journal 468 (2023). https://doi.org/10.1016/j.cej.2023.143673.

[36] M. Reig, C. Valderrama, O. Gibert, J.L. Cortina, Selectrodialysis and bipolar membrane electrodialysis combination for industrial process brines treatment: Monovalent-divalent ions separation and acid and base production, Desalination 399 (2016) 88–95. https://doi.org/10.1016/j.desal.2016.08.010.

[37] C. Morgante, F. Vassallo, C. Cassaro, G. Virruso, D. Diamantidou, N. Van Linden, A. Trezzi, C. Xenogianni, R. Ktori, M. Rodriguez, G. Micale, D. Xevgenos, Pioneering minimum liquid discharge desalination: A pilot study in Lampedusa Island, Desalination 581 (2024). https://doi.org/10.1016/j.desal.2024.117562.

[38] G. Virruso, C. Cassaro, A. Culcasi, A. Cipollina, A. Tamburini, I.D.L. Bogle, G.D.M. Micale, Multi-scale modelling of an electrodialysis with bipolar membranes pilot plant and economic evaluation of its potential, Desalination 583 (2024) 117724. https://doi.org/10.1016/j.desal.2024.117724.

[39] C. Cassaro, G. Virruso, A. Cipollina, A. Fagiolini, A. Tamburini, G. Micale, Coupling Electrodialysis with bipolar membranes with renewable energies through advanced control strategies, 2024. https://doi.org/10.1016/B978-0-443-28824-1.50330-6.

[40] A. Culcasi, L. Gurreri, A. Zaffora, A. Cosenza, A. Tamburini, G. Micale, On the modelling of an Acid/Base Flow Battery: An innovative electrical energy storage device based on pH and salinity gradients, Appl Energy 277 (2020) 115576. https://doi.org/10.1016/j.apenergy.2020.115576.

[41] H. Strathmann, J.J. Krol, H.-J. Rapp, G. Eigenberger, Limiting current density and water dissociation in bipolar membranes, J Memb Sci 125 (1997) 123–142. https://doi.org/10.1016/S0376-7388(96)00185-8.

[42] M. Herrero-Gonzalez, J. López, G. Virruso, C. Cassaro, A. Tamburini, A. Cipollina, J.L. Cortina, R. Ibañez, G. Micale, Analysis of Operational Parameters in Acid and Base Production Using an Electrodialysis with Bipolar Membranes Pilot Plant, Membranes (Basel) 13 (2023). https://doi.org/10.3390/membranes13020200.